Room temperature inorganic polycondensation of oxide (Cu2O and ZnO) nanoparticles and thin films preparation by the dip-coating technique

Guillaume Salek, Christophe Tenailleau, Pascal Dufour, Sophie Guillemet-Fritsch

▶ **To cite this version:**

Guillaume Salek, Christophe Tenailleau, Pascal Dufour, Sophie Guillemet-Fritsch. Room temperature inorganic polycondensation of oxide (Cu2O and ZnO) nanoparticles and thin films preparation by the dip-coating technique. Thin Solid Films, 2015, vol. 589, pp. 872-876. 10.1016/j.tsf.2015.04.082 . hal-01455502

HAL Id: hal-01455502
https://hal.science/hal-01455502v1

Submitted on 3 Feb 2017

HAL is a multi-disciplinary open access archive for the deposit and dissemination of scientific research documents, whether they are published or not. The documents may come from teaching and research institutions in France or abroad, or from public or private research centers.

L'archive ouverte pluridisciplinaire **HAL**, est destinée au dépôt et à la diffusion de documents scientifiques de niveau recherche, publiés ou non, émanant des établissements d'enseignement et de recherche français ou étrangers, des laboratoires publics ou privés.

Open Archive TOULOUSE Archive Ouverte (OATAO)
OATAO is an open access repository that collects the work of Toulouse researchers and makes it freely available over the web where possible.

This is an author-deposited version published in : http://oatao.univ-toulouse.fr/
Eprints ID : 16791

To link to this article : DOI : 10.1016/j.tsf.2015.04.082
URL : http://dx.doi.org/10.1016/j.tsf.2015.04.082

To cite this version : Salek, Guillaume and Tenailleau, Christophe and Dufour, Pascal and Guillemet-Fritsch, Sophie *Room temperature inorganic polycondensation of oxide (Cu2O and ZnO) nanoparticles and thin films preparation by the dip-coating technique.* (2015) Thin Solid Films, vol. 589. pp. 872-876. ISSN 0040-6090

Any correspondence concerning this service should be sent to the repository administrator: staff-oatao@listes-diff.inp-toulouse.fr

http://dx.doi.org/10.1016/j.tsf.2015.04.082

Room temperature inorganic polycondensation of oxide (Cu_2O and ZnO) nanoparticles and thin films preparation by the dip-coating technique

G. Salek, C. Tenailleau *, P. Dufour, S. Guillemet-Fritsch

Centre Interuniversitaire de Recherche et d'Ingénierie des MATériaux (CIRIMAT), UMR CNRS 5085, Université de Toulouse — UPS, 118 route de Narbonne, 31062 Toulouse Cedex 09, France

Keywords:
Cuprous oxide
Cuprite
Zinc oxide
Precipitation method
Colloidal suspension
Optical properties
Thin films

A B S T R A C T

Oxide thin solid films were prepared by dip-coating into colloidal dispersions of oxide nanoparticles stabilized at room temperature without the use of chelating or complex organic dispersing agents. Crystalline oxide nanoparticles were obtained by inorganic polycondensation and characterized by X-ray diffraction and field emission gun scanning electron microscopy. Water and ethanol synthesis and solution stabilization of oxide nanoparticle method was optimized to prepare two different structural and compositional materials, namely Cu_2O and ZnO. The influence of hydrodynamic parameters over the particle shape and size is discussed. Spherical and rod shape nanoparticles were formed for Cu_2O and ZnO, respectively. Isoelectric point values of 7.5 and 8.2 were determined for cuprous and zinc oxides, respectively, after zeta potential measurements. A shear thinning and thixotropic behavior was observed in both colloidal sols after peptization at pH ~6 with dilute nitric acid. Every colloidal dispersion stabilized in a low cost and environmentally friendly azeotrope solution composed of 96 vol.% of ethanol with water was used for the thin film preparation by the dip-coating technique. Optical properties of the light absorber cuprous oxide and transparent zinc oxide thin solid films were characterized by means of transmittance and reflectance measurements (300–1100 nm).

1. Introduction

Cuprous oxide and zinc oxide are non-toxic, low-cost, chemically stable compounds that contain abundant elements. Cuprous oxide and zinc oxide are interesting materials individually and when combined, and are thus used for various types of applications mainly due to their unique semiconductor and optical properties.

Cuprous oxide (Cu_2O) is a *p*-type conducting oxide with a direct band gap of 2.2 eV suitable for sunlight absorbance [1]. Cu_2O has attracted much attention for decades, in particular due to its potential uses in solar cells [2], photocatalysis [3], photoelectrochemical water splitting [4], transistors [5], and thin films for gas sensing [6].

Zinc oxide (ZnO) is an *n*-type conducting material with a large direct band gap of 3.4 eV [7]. The recent development of ZnO based nanomaterials and thin films has boosted research on making it suitable in shape, size and morphology for solar cells [8,9], light emitting diodes [10], microwave absorbers [11], gas sensors [12,13], piezoelectric transducers [14], and varistors [15].

Oxide thin films can be prepared by different techniques such as physical or chemical vapor deposition [16–18], spray pyrolysis [19], sputtering [20,21], electrodeposition [22,23] and sol–gel [24,25]. The latter technique is a simple and cost efficient engineering process well suited for preparing substrate coatings with controlled physical and chemical properties at low temperature. The sol–gel method usually requires surfactant or complex organic agents for preparing stable colloidal suspensions (or sols) of materials which can then be used for thin layers deposition [26,27]. Inorganic polycondensation of oxide nanoparticles is a soft-chemistry method which consists of the salts dissociation in aqueous medium with a precipitating agent such as lithium hydroxide. This method usually involves the preparation of an organometallic precursor [28]. With optimized conditions, such oxide nanoparticles can then be stabilized in a homogeneous suspension when superficial electrical charges are formed at the surface of nanoparticles due to a dispersing agent with appropriate dipolar forces. We here report on a low-cost and complex agent-free synthesis and sol stabilization of Cu_2O and ZnO nanoparticles obtained at room temperature. Cu_2O and ZnO thin films were then prepared by the dip-coating technique and their microstructural and optical properties studied.

2. Experimental details

2.1. Sample preparation

$Zn(NO_3)_2 \cdot 6H_2O$ (99% purity, purchased from PROLABO) or $CuSO_4 \cdot 5H_2O$ (99%, VWR) dissolved in pure distilled water (0.03 mol, 100 mL) were rapidly poured (5.5 L/s) at room temperature into a dilute buffered solution of LiOH (n = 0.1 mol, V = 1400 mL). After 30 min of stirring, the precipitate was washed with deionized water to remove residual ions (OH^-, Li^+ and SO_4^{2-}). An additional step consisting of reducing the $Cu(OH)_2$ precipitate was necessary for the formation of cuprous

* Corresponding author. Tel.: +33 561556283.
E-mail address: tenailleau@chimie.ups-tlse.fr (C. Tenailleau).

oxide. Ascorbic acid solution (0.015 mol) was quickly poured into the cuprous hydroxide precipitate diluted with water (500 mL) and was stirred for two hours at a fast stirring rate (240 rpm). The mixture was then centrifuged (4200 rpm for 10 min) and washed with distilled water. This step was repeated three times, removing the supernatant after each stage of centrifugation in order to eliminate the non-reactive and/or excess ions. This simple synthesis method requires only a quick precipitation, a few washings with water and neutralization (plus a fast reduction process for Cu_2O) in order to form pure and crystalline oxide powders at room temperature.

For the preparation of colloidal suspensions, a peptization step consisting of charging the nanoparticle surface was performed by the addition of nitric acid (68%) solution for stabilizing colloidal suspensions at pH ~6. A sonication step was applied to the solution at 35 kHz for 10 min to break apart possible aggregates formed in solution. Finally, colloidal suspensions of pure oxide phases were stabilized in an azeotrope solution composed of 96 vol.% absolute ethanol mixed with ultra-pure water after centrifugation of the peptized compounds before dip-coating with a NIMA DC small dip-coater from Lot–Oriel (withdrawal rate of 200 mm/min) for thin film preparation.

2.2. Sample characterization

X-ray diffraction patterns were recorded on a Bruker D4-Endeavor instrument (40 kV, 40 mA) with a CuKα wavelength, from 10 to 100° in 2-Theta, step size of 0.02° and 3.6 s/step scan. Field emission gun scanning electron microscopy (FEG-SEM) images were recorded on a JEOL 6700F instrument.

Film thickness analysis was performed with a Dektak 3030ST system from Veeco (1 mm scan length, low speed, 0.01 mN applied force and Valley profile).

Optical properties characterizations of the films were carried out using a PV300 instrument from Bentham after deposition on 5 mm thick commercial pre-cleaned and ready to use glass substrate (Menzel–Gläser purchased from Thermo Scientific) in the UV-Visible-NIR regions.

3. Results and discussion

3.1. Precipitation of oxide nanoparticles

X-ray diffraction analysis showed that pure zinc oxide of wurtzite structural type (with $P6_3mc$ space group) is formed after precipitation and the cupric hydroxide phase ($Cmc2_1$ space group) is observed in the copper based synthesis (Fig. 1). When raw cupric salt is used for the sample preparation, the copper ions possess a + II oxidation state. The ascorbic acid ($C_6H_8O_6$) was then used as a reducing agent in order to promote the following two reactions and form the cuprous oxide:

$$Cu(OH)_2 + C_6H_8O_6 = Cu^{2+} + C_6H_6O_6^{2-} + 2H_2O$$

$$2\,Cu^{2+} + C_6H_6O_6^{2-} + H_2O = Cu_2O + C_6H_6O_6 + 2\,H^+.$$

Shape control mechanism of cuprous oxide nanoparticles was recently studied in aqueous solutions with the use of a polyvinylpyrrolidone surfactant [29]. Size and low-dimensional structures are governed by thermodynamic and kinetic parameters. A supersaturated medium containing a large excess of ascorbic acid will drive the reaction to the formation of Cu_2O nanoparticles of cubic shape (200 nm average diameter size). But large excess of ascorbic acid (twice the amount of reactant) can be too reducing and metal copper is usually formed after stirring for half an hour or more. The particle morphology is also sensitive to the stirring rate. A fast stirring rate strongly increases the probability of collisions between particles and can lead to the formation of nanospheres [29]. Here, the quick addition of the ascorbic acid solution into the cuprous hydroxide precipitate at a fast stirring rate allows the formation of spherical cuprous oxide nanospheres with the cuprite structure (*Pn-3m* space group) by a successive dissolution/reprecipitation mechanism (Figs. 1c and 2a). Monodisperse solutions contain particles with an average size of 84 ± 21 nm. Larger spheres of Cu_2O can be obtained when equivalent molar numbers of Cu^{2+} and OH^- (n = 0.03 mol) and volumes of salt and alkaline solutions are used during the precipitate formation step (see Fig. 2b).

Micrometer flakes or nanorod-like particles of zinc oxide are formed depending on the nature of the solvent used during the synthetic process (Fig. 3). When the solvent used during precipitation is water crystal plates will assemble together to form flakes (Fig. 3a), that can be eventually broken apart by sonication (Fig. 3b), while a mixture of 70 vol.% of water and 30 vol.% of alcohol leads to uniquely zinc oxide nanorods (Fig. 3c). The nature of the solvent can indeed influence the mechanism of nucleation [30]. Particle shape obtained during precipitation depends on the number of hydrogen bonds offered by the solvent. Solvent molecules can considerably modify the sample stability and agglomeration phenomenon. Moreover, the germination and growth processes, which are governed by the degree of supersaturation and interfacial energy, can be strongly modified by the change of solvent [31,32]. The oxide particles morphology also strongly depends on the dielectric constant of the aqueous medium. A mixed solution of water and ethanol with

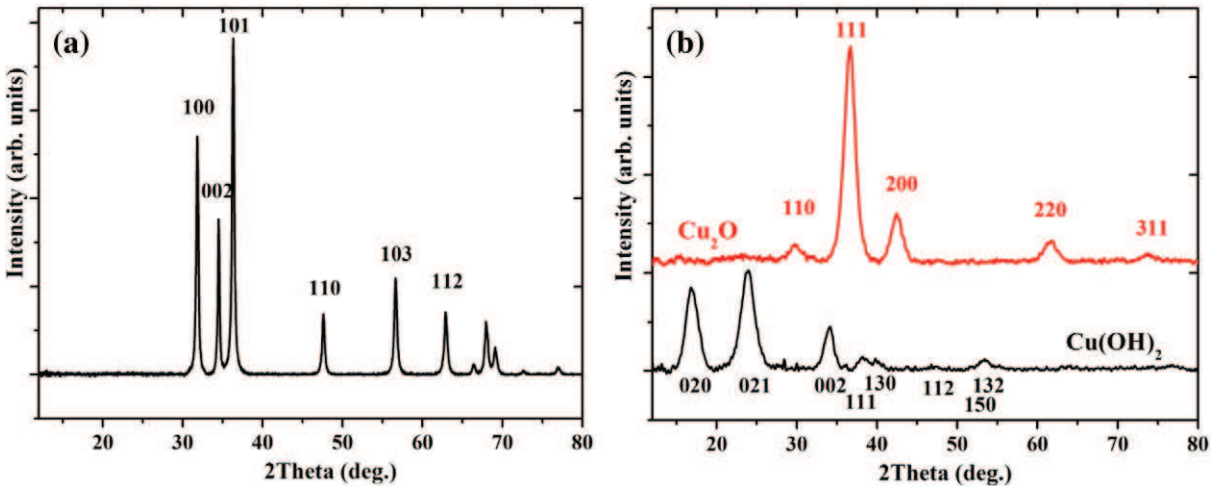

Fig. 1. X-ray diffraction patterns of zinc oxide (left) and copper hydroxide (bottom right) obtained after precipitation. In the latter case, ascorbic acid was used to form crystalline cuprous oxide (top right). Miller indices are given for the first main diffraction peaks.

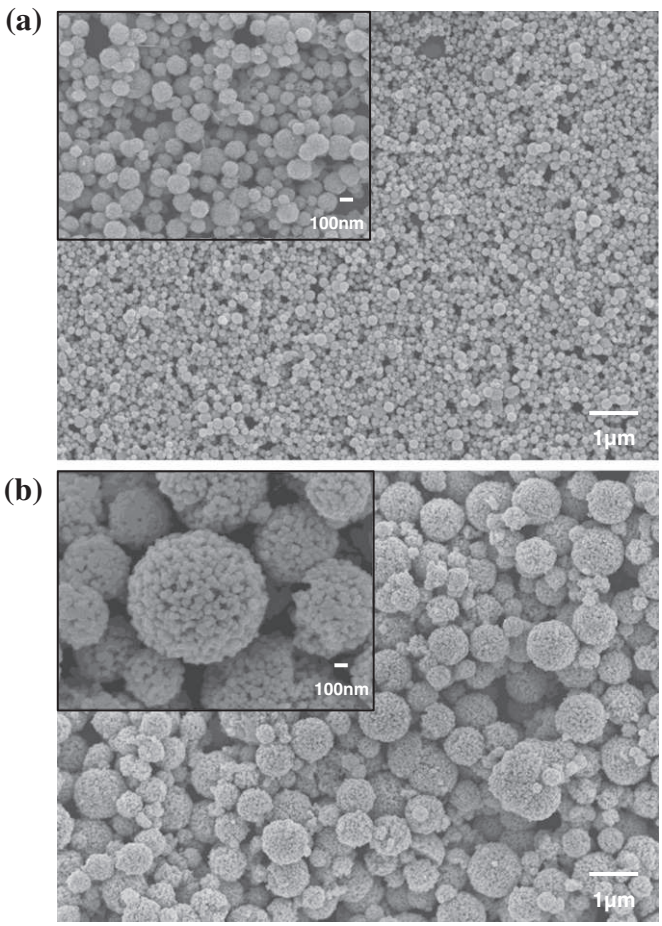

Fig. 2. Scanning electron microscopy images of Cu_2O nanoparticles in the case of excess (a) and (b) equimolar ratio of (ascorbic acid/solution salt) used to form the precipitate.

decreased dielectric constant, influence the growth process along a special crystallographic axis which leads to single rod-like shaped nanoparticles (Fig. 3c).

3.2. Sol stabilization

It is well known that zinc oxide and cuprous oxide are sensitive to dissolution in aqueous solutions at ambient temperature. This phenomenon closely depends on the chemical species present in solution. Pourbaix diagrams are often used to view the equilibrium chemistry of a species in terms of redox behavior or solubility alone [33]. Their stabilization in aqueous medium by modification of their hydroxyl groups with inorganic acids is only possible in a small specific pH region. For zinc oxide, at ambient temperature and in acid medium (pH < 6), the dissolution is in principle due to the direct attack of protons on the particles surface. This promotes the formation of the soluble forms $Zn(OH)^+$ [34,35]. In alkaline media (pH > 9), the dissolution phenomenon is generally attributed to the formation of different hydroxyl ions such as $Zn(OH)_3^-$ and $Zn(OH)_4^{2-}$ [34, 36]. Similarly, for cuprous oxide under acidic conditions, the solubility is closely related to the chemical species with which copper can form complexes [37]. Similarly, following the Pourbaix diagram for copper oxide stabilization, Cu^+ is formed in slightly acid solution (pH ~5–6), in a small potential area compared to Cu^{2+}, without any complexing agent. $Cu^{II}(OH)_2$ and $Cu^{I}(OH)$ are predominant in water under mildly alkaline conditions (pH > 9) and their presence also depends on the oxygen solubility in water [33,37].

Zeta potential measurements showed an isoelectric point value of 7.5 and 8.2 for Cu_2O and ZnO, respectively (Fig. 4). Zeta potential is maximum at a pH value close to 6. Zeta potential decrease observed either at

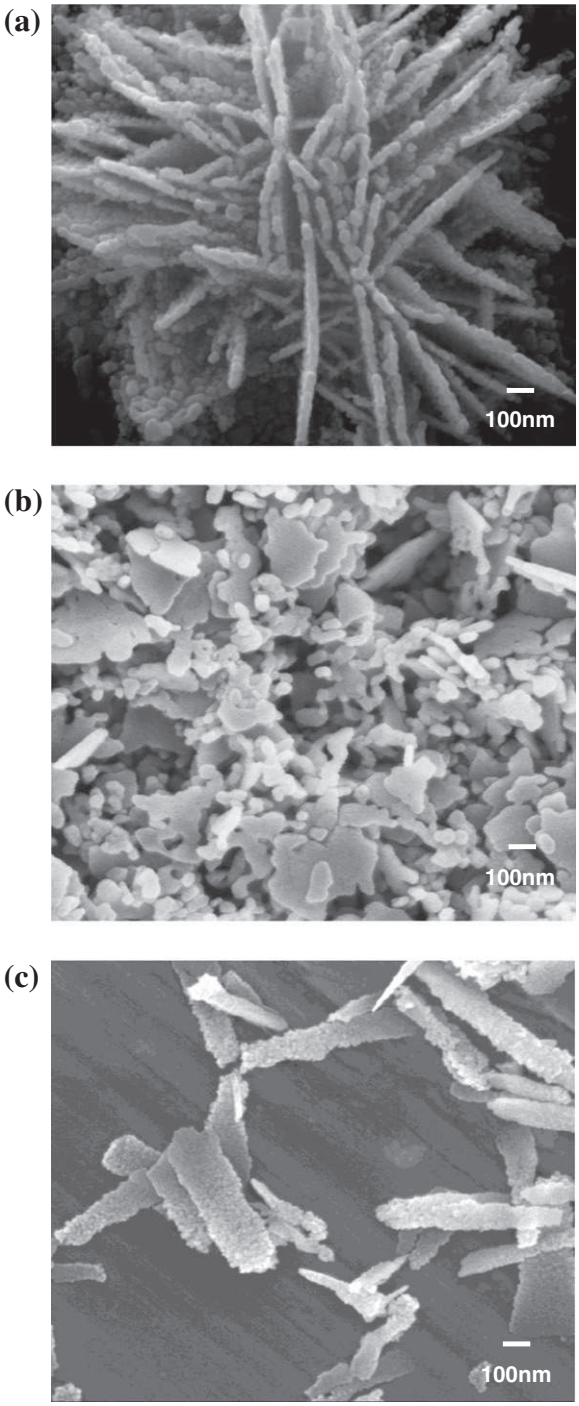

Fig. 3. Scanning electron microscopy images of ZnO nanoparticles.

lower or higher pH could be explained by a partial dissolution of the particles of ZnO and Cu_2O. At this range of pH, the increase of ionic strength by dissolution of particles could induce a compression of the ionic double layer of particles thus changing the size of the agglomerate mobility.

Therefore, a short strong ultrasonication (35 kHz for 5 min) coupled with the addition of an acidic solution of dilute nitric acid (pH ~6) was utilized to disperse and stabilize the particles in solution. After this step of peptization/deagglomeration, an azeotrope mixture containing 96 vol.% of absolute ethanol and 4 vol.% of ultrapure water was used to obtain the final sol, allowing the stabilization of particles and improving the wettability of the sol on a glass substrate. The viscosity variations of this sol as a function of the shear strain is given in Fig. 5 for each oxide

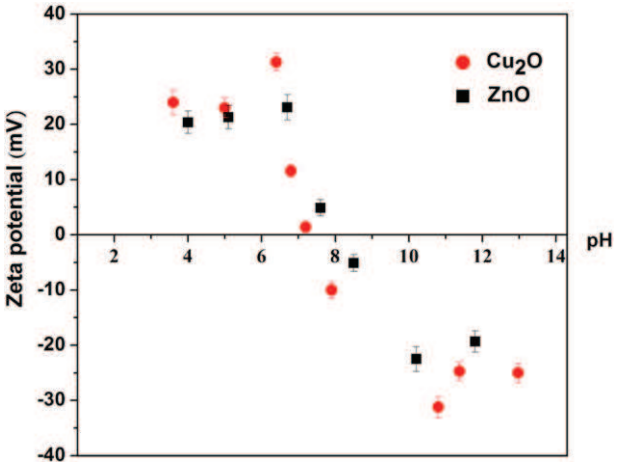

Fig. 4. Zeta potential measurements vs pH for ZnO (squares) and Cu_2O (circles).

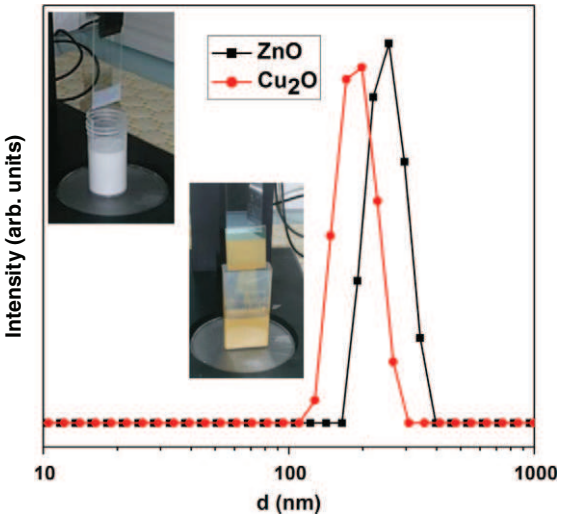

Fig. 6. Particles granulometry distributions in colloidal dispersions of zinc oxide (squares) and cuprous oxide (circles).

colloidal dispersion. Both dispersions of Cu_2O and ZnO exhibit a rheofluidifying (pseudo-plastic) and slightly thixotropic behavior as shown by the non-linearity of the curves and the presence of a small hysteresis. Particle granulometric distributions in colloidal dispersions were measured by dynamic light scattering after ultrasonication of each solution at 35 kHz for 10 min. Cuprous oxide and zinc oxide solutions exhibit a narrow distribution of aggregates with an average particle diameter centered around 198 and 255 ± 5 nm, respectively (Fig. 6). Solutions of ZnO were stable for a couple of weeks while colloidal dispersions of Cu_2O were stable for a few months.

3.3. Oxide thin films preparation and their optical properties

Oxide thin films of Cu_2O and ZnO were prepared by dip-coating into the corresponding colloidal dispersions. Contact profilometry measurements showed that a thin layer of ~300 nm can be obtained after one dip-coating sequence for both compounds, although particle shapes are different for Cu_2O (spheres) and ZnO (rods).

Fig. 7 shows room temperature transmittance and reflectance data and insets are FEG-SEM images of a micrometer thick and homogeneous oxide layer obtained after three successive dip-coatings. Optical features are identical for 300 nm thin layers of oxides. Absorbance curves were deduced by summing all three contributions to 100%.

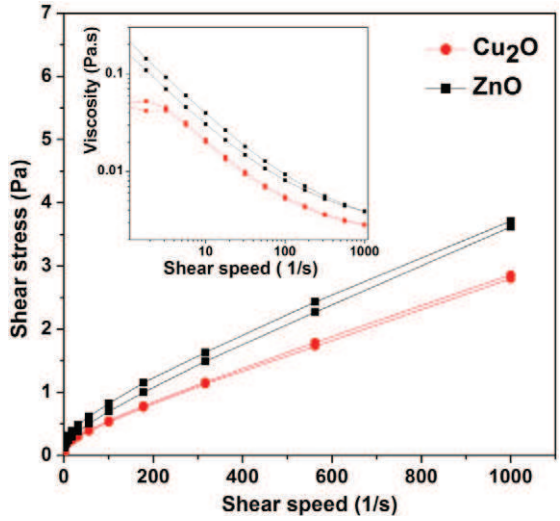

Fig. 5. Shear stress variation as a function of the shear strain for a colloidal dispersion of zinc oxide (squares) and cuprous oxide (circles). Inset shows the viscosity variation vs shear speed.

A strong absorption edge is observed for the orange/red Cu_2O thin films, from the UV region to the low wavelengths of the visible region. In the cuprous oxide, the top part of the valence band does not only constitute oxygen orbitals, as it is usually observed for transition metal oxides, but contains also fully occupied metal d orbitals [38–40]. The Cu^+ ions 4 s^0 orbitals correspond to the conduction band lower energy levels and charge transfer can occur from the hybridized orbitals forming the valence band to the empty Cu states at the conduction band. The optical direct band gap value of ~2.4 eV, which was determined following Tauc's equation [41], is higher than the band gap (~2 eV) measured in Cu_2O films grown by electrodeposition technique [42]. The higher band gap observed in our work can be related to a quantum confinement effect due to smaller particle sizes [43]. Indeed, the average crystallite size is approximately 10 nm in diameter, as determined by Scherrer's law from the X-ray diffraction patterns, but even smaller particles (below 5 nm) can also be seen in SEM images, supporting the assumption of quantum confinement effect.

ZnO thin films are highly transparent over the visible-NIR region. A direct energy band gap of 3.3 eV for ZnO was determined by extrapolation of the vertical line calculated following Tauc's equation [41], in accordance with the literature [7].

These homogeneous thin films of Cu_2O and ZnO obtained at room temperature by the dip-coating method after a strict control of the parameters for the precipitation process and sol dispersion stabilization needed to be sintered to form compact layers. The two materials could then be combined for various applications including photovoltaics. Finally, this water and ethanol synthesis and solution stabilization of oxide nanoparticle method have proven to be efficient for the preparation of thin and crystallized oxide solid films at room temperature, and can thus be extended to a large variety of target structures.

4. Conclusions

Monodisperse distributions of oxide particles were stabilized in colloidal dispersions using a simple and low cost method that was optimized at room temperature using only water and ethanol as solvents. Cu_2O nano- or micro-particles are spherical and their size can be adjusted by changing the proportions of metal salts and alkaline solutions.

Two types of ZnO particle morphology, flakes or rods, were synthetized by modification of the dielectric constant of the solvent.

After peptization at pH ~6, oxide colloidal suspensions were stabilized in an azeotrope ethanol mixed water solution. The small size of hydrodynamic particles and the high positive zeta potential used to

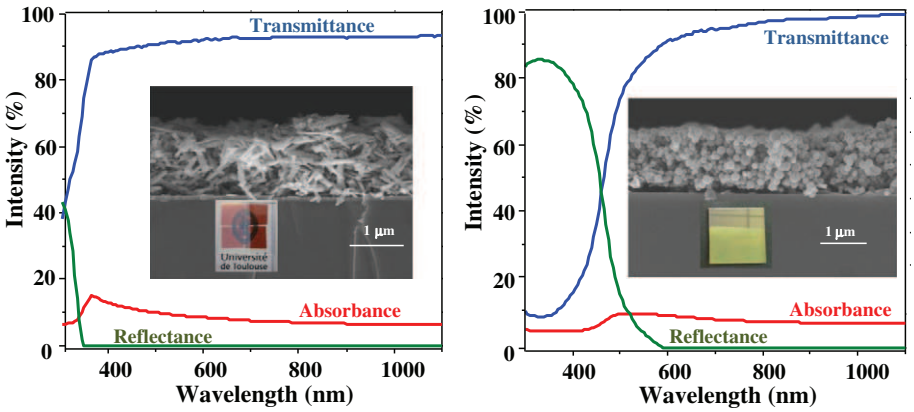

Fig. 7. Transmittance, reflectance and deduced absorbance spectra of ZnO (left) and Cu_2O (right) measured on thin films at room temperature. Insets show side cuts scanning electron microscopy images and top views of three oxide layers deposited on glass substrates for both materials.

stabilize our sols allow the formation of stable suspensions which exhibit a rheofluidifiant behavior. As-prepared dispersions were then used for the oxide thin films preparation by the dip-coating technique. Homogeneous thin films (~300 nm after one dip-coating sequence) of oxides were formed on glass substrates. The dark orange cuprous oxide films strongly absorb in the UV region and low wavelengths of the visible region while the whitish zinc oxide films are transparent from the UV to the IR regions.

Acknowledgments

This work was supported by the French Ministry of Education and Research. Isabelle Pasquet and Jean-Jacques Demai are thanked for their assistance in recording the SEM images.

References

[1] M.Y. Shen, T. Yokouchi, S. Koyama, T. Goto, Dynamics associated with Bose–Einstein statistics of orthoexcitons generated by resonant excitations in cuprous oxide, Phys. Rev. B 56 (1997) 13066.
[2] H.M. Wei, H.B. Gong, L. Chen, M. Zi, B.Q. Cao, Photovoltaic efficiency enhancement of Cu_2O solar cells achieved by controlling homojunction orientation and surface microstructure, J. Phys. Chem. C 116 (2012) 10510.
[3] Y. Zhang, B. Deng, T. Zhang, D. Gao, A.-W. Xu, Shape effects of Cu_2O polyhedral microcrystals on photocatalytic activity, J. Phys. Chem. C 114 (2010) 5073.
[4] M. Hara, T. Kondo, M. Komoda, S. Ikeda, J.N. Kondo, K. Domen, M. Hara, K. Shinohara, A. Tanaka, Cu_2O as a photocatalyst for overall water splitting under visible light irradiation, Chem. Commun. 2 (1998) 357.
[5] E. Fortunato, V. Figueiredo, P. Barquiha, E. Elamurugu, P. Barros, G. Gongcalves, S.H.K. Park, C.S. Hwang, R. Martins, Thin-film transistors based on p-type Cu_2O thin films produced at room temperature, Appl. Phys. Lett. 96 (2010) 192102.
[6] P.A. Praveen Janantha, L.N.L. Perera, K.M.D.C. Jayathilaka, J.K.D.S. Jayanetti, D.P. Dissanayaka, W.P. Siripala, Use of Cu_2O microcrystalline thin film semiconductors for gas sensing, Proc. Tech. Sessions 25 (2009) 70.
[7] R. Hauschild, H. Priller, M. Decker, J. Brückner, H. Kalt, C. Klingshirn, The exciton polariton model and the diffusion of excitons in ZnO analyzed by time-dependent photoluminescence spectroscopy, Phys. Status Solidi C 3 (4) (2006) 980.
[8] J. Wu, G. Chen, H. Yang, C. Ku, J. Lai, Effects of dye adsorption on the electron transport properties in ZnO-nanowire dye-sensitized solar cells, Appl. Phys. Lett. 90 (2007) 2131091.
[9] M. Igalson, C. Platzer-Björkman, The influence of buffer layer on the transient behavior of thin film chalcopyrite devices, Sol. Energy Mater. Sol. Cells 84 (2004) 93.
[10] K. Kim, J.S. Horwitz, W.H. Kim, A.J. Makinen, Z.H. Kafafi, D.B. Chrisey, Doped ZnO thin films as anode materials for organic light-emitting diodes, Thin Solid Films 420–421 (2002) 539.
[11] Z.W. Zhou, W.M. Peng, S.Y. Ke, H. Deng, Tetrapod-shaped ZnO whisker and its composites, J. Mater. Process. Technol. 89–90 (1999) 415.
[12] J. Chen, J. Lin, J. Li, G. Xiao, X. Yang, Large-scale syntheses of uniform ZnO nanorods and ethanol gas sensors application, J. Alloys Compd. 509 (2011) 740.
[13] S.J. Pearton, D.P. Norton, K. Ip, Y.W. Heo, Recent progress in processing and properties of ZnO, T. Steiner, Prog. Mater. Sci. 50 (2005) 293.
[14] S.C. Ko, Y.C. Kim, S.S. Lee, S.H. Choi, S.R. Kim, Micromachined piezoelectric membrane acoustic device, Sensors Actuators A Phys. 103 (2003) 130.
[15] L. Saint Macary, M.L. Kahn, C. Estournès, P. Fau, D. Trémouilles, M. Bafleur, P. Renaud, B. Chaudret, Size effect on properties of varistors made from zinc oxide nanoparticles through low temperature spark plasma sintering, Adv. Funct. Mater. 19 (2009) 1775.
[16] J. Kouam, T. Ait-Ahcene, A.G. Plaiasu, M. Abrudeanu, A. Motoc, E. Beche, C. Monty, Characterization and properties of ZnO based nanopowders prepared by solar physical vapor deposition (SPVD), Sol. Energy 82 (2008) 226.
[17] X.H. Wang, R.B. Li, D.H. Fan, Control growth of catalyst-free high-quality ZnO nanowire arrays on transparent quartz glass substrate by chemical vapor deposition, Appl. Surf. Sci. 257 (2011) 2960.
[18] G. Gugliettaa, T. Wangaa, R. Patib, S. Ehrmanb, R.A. Adomaitisa, Chemical vapor deposition of copper oxide films for photoelectrochemical hydrogen production, in: Frank E. Osterloh (Ed.),Proc. of SPIE, Solar Hydrogen and Nanotechnology IV, 7408 2009, p. 7408071.
[19] R. Ayouchi, D. Leinen, F. Martin, M. Gabas, E. Dalchiele, J.R. Ramos-Barrado, Preparation and characterization of transparent ZnO thin films obtained by spray pyrolysis, Thin Solid Films 426 (2003) 68.
[20] J.R. Ray, M.S. Desai, C.J. Panchal, P.B. Patel, Magnetron sputtered Al–ZnO thin films for photovolataic applications, J. Nano. Electron. Phys. 3 (2011) 755.
[21] S. Izhizuka, S. Kato, T. Maruyama, K. Akimoto, Nitrogen doping into Cu_2O thin films deposited by reactive radio–frequency magnetron sputtering, Jpn. J. Appl. Phys. 40 (2001) 2765.
[22] S. Sanchez, D. Aldakov, D. Rouchon, L. Rapenne, A. Delamoreanu, C. Lévy-Clément, V. Ivanova, Sensitization of ZnO nanowire arrays with CuInS2 for extremely thin absorber solar cells, J. Renewable Sustainable Energy 5 (2013) 011207.
[23] K. Mukhopadhyay, A.K. Chakroborty, A.P. Chatterjee, S.K. Lahiri, Galvanostatic deposition and characterization of cuprous oxide thin films, Thin Solid Films 209 (1992) 92.
[24] C.D. Bojorge, H.R. Canepa, U.E. Gilabert, D. Silva, E.A. Dalchiele, R.E. Marotti, Synthesis and optical characterization of ZnO and ZnO:Al nanocrystalline films obtained by the sol–gel dip-coating process, J. Mater. Sci. Mater. Electron. 18 (2007) 1119.
[25] H.Y. Xu, C. Chen, L. Xu, J.K. Dong, Direct growth and shape control of Cu_2O film via one-step chemical bath deposition, Thin Solid Films 527 (2013) 76.
[26] A.K. Kyaw, X.W. Sun, C.Y. Jiang, Efficient charge collection with sol–gel derived colloidal ZnO thin film in photovoltaic devices, J. Sol-Gel Sci. Technol. 52 (2009) 348.
[27] L. Znaidi, Sol–gel-deposited ZnO thin films: a review, Mater. Sci. Eng. B 174 (2010) 18.
[28] L. Spanhel, M.A. Anderson, Semiconductor clusters in the sol–gel process: quantized aggregation, gelation, and crystal growth in concentrated zno colloids, J. Am. Chem. Soc. 113 (1991) 2826.
[29] Y. Bai, T. Yang, Q. Gu, G. Cheng, R. Zheng, Shape control mechanism of cuprous oxide nanoparticles in aqueous colloidal solutions, Powder Technol. 227 (2012) 35.
[30] A.E. Nielsen, Precipitation, Croat. Chem. Acta 42 (1970) 319.
[31] C. Marcilly, Revue de l'Institut Français du Pétrole, 391984. 189.
[32] G. Charlot, B. Tremillon, Les réactions chimiques dans les solvants et les sels fondus, Gauthier-Villars, Paris, 1963.
[33] M. Pourbaix, Atlas of Electrochemical Equilibria in Aqueous Solutions, Pergamon, New York, 1966.
[34] S. Yamabi, H. Imai, Growth conditions for wurtzite zinc oxide films in aqueous solutions, J. Mater. Chem. 12 (2002) 3773.
[35] A. Degen, M Kosec, Effect of pH and impurities on the surface charge of zinc oxide in aqueous solution, J. Eur. Ceram. Soc. 20 (2000) 667.
[36] S.W. Bian, I.A. Mudunkotuwa, T. Rupasinghe, V.H. Grassian, Aggregation and dissolution of 4 nm ZnO nanoparticles in aqueous environments: influence of pH, ionic strength, size, and adsorption of humic acid, Langmuir 27 (2011) 6059.
[37] D.A. Palmer, Solubility measurements of crystalline Cu_2O in aqueous solution as a function of temperature and pH, J. Solut. Chem. 40 (2011) 1067.
[38] L. Zhang, L. McMillon, J. McNatt, Gas-dependent bandgap and electrical conductivity of Cu2O thin films, Sol. Energy Mater. Sol. Cells 108 (2013) 230.
[39] Y. Nakano, S. Saeki, T. Morikawa, Optical bandgap widening of p -type Cu_2O films by nitrogen doping, Appl. Phys. Lett. 94 (2009) 2008.
[40] J.P. Hu, D.J. Payne, R.G. Egdell, On-site interband excitations in resonant inelastic x-ray scattering from Cu_2O, Phys. Rev. B 155115 (2008) 1.
[41] J. Tauc, Optical properties and electronic structure of amorphous Ge and Si, Mater. Res. Bull. 3 (1968) 37.
[42] W. Siripala, L.D.R.D. Perera, K.T.L. De Silva, J.K.D.S. Jayanetti, Study of annealing effects of cuprous oxide grown by electrodeposition technique, Sol. Energy Mater. Sol. Cells 44 (1996) 251.
[43] P. He, X. Shen, H. Gao, Size-controlled preparation of Cu_2O octahedron nanocrystals and studies on their optical absorption, J. Colloid Interface Sci. 284 (2005) 510.